Chapter 2

# Design of Energy Management System of a PEMFC–Battery–Supercapacitor Hybrid Tramway

Qi Li and Weirong Chen

Additional information is available at the end of the chapter

http://dx.doi.org/10.5772/64696

**Abstract**

In this chapter, a hybrid power system that consists of multiple proton exchange membrane fuel cell (PEMFC) systems, batteries, and supercapacitors (SCs) is developed for a hybrid tramway. Three energy management strategies that included a fuzzy logic control (FLC), an equivalent consumption minimization strategy (ECMS), and a state machine strategy based on droop control (SMS-DC) are utilized to coordinate multiple power sources, avoid the transients and rapid changes of power demand, and achieve high efficiency without degrading the mechanism performance for an energy management system of hybrid tramway. A hybrid system model of tramway is established with commercially available devices, and then the different energy management strategies are evaluated with a real driving cycle of tramway from Turkey. The results compared with these strategies demonstrate that the higher average efficiencies of the tramway, the lower tramway-equivalent hydrogen consumptions, and more efficient use of the batteries and SCs energy are achieved by the SMS-DC. Therefore, the appropriate energy management system for high-power hybrid tramway will improve the hydrogen consumptions of overall hybrid system and the efficiencies of each power source.

**Keywords:** proton exchange membrane fuel cell, hybrid tramway, energy management system, a state machine strategy, fuzzy logic control, equivalent consumption minimization strategy

## 1. Introduction

Nowadays, environmental issues and energy crisis relating to oil supply, pollution, and green house effects justify the need for developing of new technologies for transportation. Fuel cells as a promising technology, which provide electrical power with high efficiency, less noise, and

near zero emissions compared with conventional internal combustion engines, are expected to become a viable solution for transportation applications [1, 2]. Due to its lower operating temperature and higher efficiency, a proton exchange membrane fuel cell (PEMFC) is considered as one of the most prime candidates for the vehicular applications [3–5].

In recent years, several research efforts have been carried out to develop the locomotives and the tramways powered by the PEMFC in order to encourage hydrogen economy development and reduce dependence on fossil fuels [6–12]. The locomotives and the tramways powered by the PEMFC and the energy storage system (ESS) contrasted with the diesel-electric and catenary-electric types have many advantages, which show great extensive application potential. The PEMFC exhibits good power capability during steady-state operation, but its response limitation for transient peak power demand has restrained the PEMFC from being used in large-scale and high-power transportation applications, and the lifetime of the PEMFC may be dramatically impacted by the rapid power demand variations. Due to the unidirectional power flow characteristics of the PEMFC, the energy from regenerative braking of a vehicle cannot be handled by the PEMFC. Hence, hybridizing the PEMFC with the ESS, such as battery, supercapacitor (SC), or a combination of both, can meet the total power demand and reduce the effect of drawback from the powertrain driven by stand-alone PEMFC. The hybrid tramway composed of multiple motor and trailer units, such as the type of two motor units and one trailer unit, is driven by multiple PEMFC and ESS based on the requirement of the power level and the mounting space. In order to fulfill the power balance between the load power demand and the power sources, the energy flows are distributed by the energy management system, which determines the power generation split at each sampling time between the PEMFC and the ESS, such as battery and SC.

Recently, the development of energy management system has become a topic of interest for researchers. Jia et al. [4] have presented the electrical characteristic of a hybrid power supply system combining PEMFC and SC and have investigated on the platform of an electric bicycle to improve the system efficiency. Xu et al. [5] have proposed a multimode real-time control strategy based on three typical processes of the fuel cell system for a fuel cell electric vehicle, taking the fuel economy and system durability into consideration. Li et al. [6, 7] have proposed a power sharing strategy for an energy management system of hybrid tramway and also have presented a state machine strategy based on droop control to coordinate multiple power sources of hybrid tramway. García et al. [10] have presented an equivalent consumption minimization strategy for the energy management system of the fuel cell/battery/SC tramway. Torreglosa et al. [11] have optimized the tramway hydrogen consumption based on fuel cell/battery hybrid system by the equivalent consumption minimization strategy. Fernandez et al. [12] have utilized a state machine control to satisfy the power demand from the real driving cycle for the fuel cell/battery hybrid tramway. Thounthong et al. [13] have fulfilled the comparisons between linear proportional integral and nonlinear flatness-based controllers for DC link stabilization. Eren et al. [14] have proposed a fuzzy logic supervisory controller-based power management strategy that secures the power balance in hybrid structure, enhances the FC performance, and minimizes the power losses for an FC/UC hybrid vehicular power system.

http://dx.doi.org/10.5772/64696

In this chapter, a hybrid propulsion system including two PEMFC systems, two batteries, and two SCs is developed for the tramway with two motor units and one trailer unit. The PEMFC systems act as main power source of tramway, and the Li-ion batteries and the SCs are utilized as the ESS to supplement the PEMFC output power during tramway acceleration and cruise and are also utilized for energy recovery during braking. A hybrid system model of tramway is established with commercially available devices. Furthermore, three energy management strategies included a fuzzy logic control (FLC), an equivalent consumption minimization strategy (ECMS) and a state machine strategy based on droop control (SMS-DC) are utilized to coordinate and distribute the power demand from each power source of the tramway, and the comparisons are also carried out to verify the validity according to a driving cycle.

## 2. Configuration of hybrid tramway

A hybrid tramway without grid connection called LF-LRV is being developed by Chinese manufacturer of Tangshan Railway Vehicle Co. Ltd and Southwest Jiaotong University. This hybrid tramway, which presents a capacity of 360 passengers and reaches a maximum speed of 77 km/h, is composed of two motor units and one trailer unit. Two motor units are supplied by the tramway traction system via an inverter box. The proposed configuration of PEMFC–battery–SC powered hybrid tramway is shown in **Figure 1**. The hybrid powertrain is composed of the PEMFCs (manufactured by Ballard), the batteries (manufactured by Microvast Power), the SCs (manufactured by Maxwell), the unidirectional DC/DC converters, the bidirectional DC/DC converters, the traction motors, auxiliary service module, and braking resistor. The PEMFC systems (No. 1 and No. 2) and two unidirectional DC/DC converters are placed on the trailer unit. The batteries and the SCs (No. 1 and No. 2) and two bidirectional DC/DC converters are, respectively, placed on two motor units. The boost-type unidirectional DC/DC converters are used to raise the DC voltage to 750 V. Two batteries and two SCs are connected to the traction DC bus through two bidirectional DC/DC converters, respectively, which allow the charge and discharge of the batteries and the SCs. Particularly, two SCs are utilized to consume the peak power that neither the PEMFCs nor the batteries can store because of their high specific power and high dynamic response.

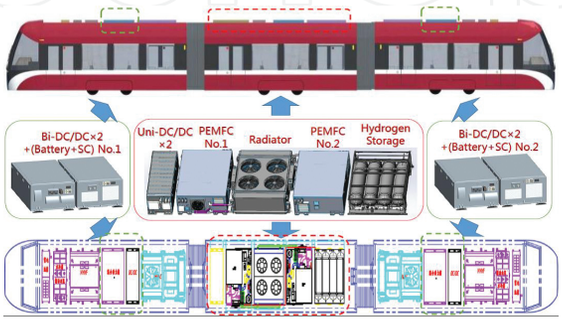


**Figure 1.** Configuration of PEMFC–battery–SC powered hybrid tramway.

## 3. Modeling of hybrid power system

### 3.1. Modeling of PEMFC power unit

A PEMFC power unit, which consists of a power module subsystem, a control subsystem, and a hydrogen storage subsystem, is considered as the heart of the hybrid power system for the tramway [6, 8]. The PEMFC power unit is setup in the clean energy laboratory of Southwest Jiaotong University. In the designed PEMFC power unit, a Ballard Stack HD6 Module-FCvelocity™ is used as the PEMFC stack module. This stack module is rated at 150 kW gross power, which contains the auxiliary components for hydrogen recirculation and purge, and air humidification. The key component for the air delivery module is the air compressor, which utilizes a turbo charger manufactured by ROTREX™ Corporation. The cooling module is fulfilled with two separate cooling loops. The primary cooling loop provides heat rejection for the HD6 Module. The second cooling subsystem provides heat rejection for the PEMFC stack module condenser to ensure enough process water available at all times for air humidification.

A model of PEMFC power unit is developed based on the 150 kW Ballard HD6 Module testing data. A set of assumptions generally undertaken in similar studies is carried out to focus on the dynamic response analysis for the HD6 Module requested current and output voltage [15–19]. The PEMFC output voltage is decreased from its equilibrium potential because of irreversible losses. Particularly, the concentration losses are neglected under practical working condition. The output voltage equation is expressed as

$$U_{\mathrm{fc}} = E_{\mathrm{oc}} - U_{\mathrm{act}} - U_{\mathrm{ohmic}} \tag{1}$$

$$\text{with} \quad \begin{cases} E_{\mathrm{oc}} = K_{\mathrm{c}}\left[E_0 + (T-298)\dfrac{-44.43}{zF} + \dfrac{RT}{zF}\ln(P_{\mathrm{H}_2}P_{\mathrm{O}_2}^{1/2})\right] \\ U_{\mathrm{act}} = \dfrac{1}{\tau s + 1} NA_{\mathrm{nom}} ln(\dfrac{i_{\mathrm{fc}}}{i_0}) \\ U_{\mathrm{ohmic}} = R_{\mathrm{internal}} i_{\mathrm{fc}} \end{cases} \tag{2}$$

where $E_{\mathrm{oc}}$ is the open circuit voltage, $U_{\mathrm{fc}}$ is the stack output voltage, $U_{\mathrm{ohmic}}$ is the ohmic voltage drop, and $U_{\mathrm{act}}$ is the activation voltage drop, $E_0$ is the electromotive forces under standard pressure, $K_{\mathrm{c}}$ rated voltage constant, $T$ is the operating temperature, $z$ is transfer electron number, $P_{\mathrm{H2}}$ and $P_{\mathrm{O2}}$ are the gas pressures, $F$ is Faraday constant, $R$ is the gas constant, $i_{\mathrm{fc}}$ is the cell output current, $R_{\mathrm{internal}}$ is inner resistance of a stack, $N$ is the number of cells, $\tau$ is the dynamic response time constant that will make the cell output voltage exhibits a delay approximately during a sudden change in cell output current. The detailed description about the modeling of the PEMFC power unit based on HD6 Module can be found in [6, 8]. In order to prove the validity of the PEMFC power unit model, the comparisons between the experimental data and

http://dx.doi.org/10.5772/64696

the characteristics curve of polarization by simulation are achieved. The polarization curve by simulation and the experimental data are in good match as shown in **Figure 2**.

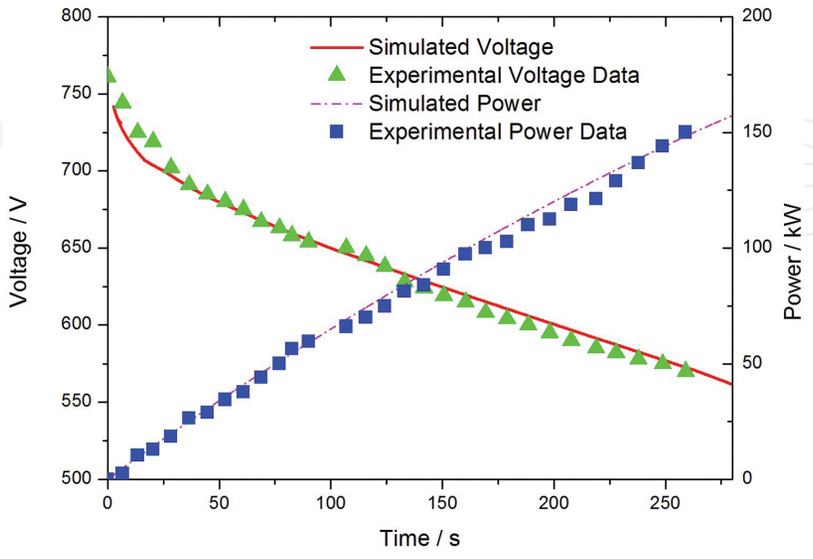


**Figure 2.** Comparisons between the experimental data and the polarization curve by simulation.

### 3.2. Modeling of energy store system

The batteries considered for the hybrid system are of type Li-ion as they have proven to exhibit high energy density and efficiency and a large number of charge/discharge cycles compared with other battery types [6, 7, 10]. The Li-ion batteries are utilized both for supplying a portion of the base load together with PEMFC and capturing the braking energy together with the SC. The behavior of this battery is represented by a modified Shepherd curve-fitting model presented in [10, 20], which is available in the SimPowerSystems toolbox of Simulink. In this model, a voltage polarization is added to the battery discharge voltage expression to better represent the effect of the battery stage of charge (SOC) on the battery performance. The validity of this model has been verified by experimental studies [20–22]. The battery SOC is calculated as follows:

$$SOC = 100[1 - \frac{1}{Q}\int_0^t i_{\text{bat}}(t)dt] \tag{3}$$

According to the battery open circuit voltage and voltage drop resulting from the battery-equivalent internal impedance, the battery output voltage can be calculated as follows:

$$U_{\text{bat}} = E_0 - K\frac{Q}{Q-it}it - R_{\text{b}}i_{bat} + A_{\text{b}}\exp(-Bit) - Pol_{\text{res}}i^* \tag{4}$$

where $E_0$ is the constant voltage, $i_{bat}$ is the battery current, $K$ is the polarization constant, $Q$ is the maximum battery capacity, $i^*$ is the filtered battery current, $it$ is the actual battery charge, $A_b$ is the exponential zone amplitude, $B$ is the exponential zone time constant inverse, and $R_b$ is the battery internal resistance. $Pol_{res}$ is the polarization resistance, which can be decided as follows:

$$Pol_{res} = K\frac{Q}{Q-it}(1-u(t)) + K\frac{Q}{it-0.1Q}u(t) \tag{5}$$

where $u$(t) is equal to 1 if battery is charging and is equal to 0 if battery is discharging. The detailed description about the modeling of the battery model can be found in [6, 7, 20].

The SC, which is known as electric double-layer capacitor, is similar to conventional electrostatic or electrolytic capacitor with the advantage that it can store or release more energy due to their high capacitance. The SC model presented in [20, 23] is available in the SimPowerSystems toolbox of Simulink. This model consists of a capacitance representing the SC performance during the charging and discharging process and an equivalent series resistance representing the charging and discharging resistance. The SC output voltage is expressed considering resistive losses as follows:

$$U_{sc} = \frac{Q_T}{C_T} - R_{sc}i_{sc} \tag{6}$$

$$\text{with} \quad \begin{cases} C_T = \dfrac{N_p}{N_s}C \\ Q_T = N_p Q_c = \int i_{sc}dt \\ C = \left(\dfrac{1}{C_H} + \dfrac{1}{C_{GC}}\right)^{-1} \\ C_H = \dfrac{N_e \varepsilon \varepsilon_0 A_i}{d} \\ C_{GC} = \dfrac{FQ_c}{2N_e RT}\sinh\left(\dfrac{Q_c}{N_e^2 A_i \sqrt{8RT\varepsilon\varepsilon_0 c}}\right) \end{cases} \tag{7}$$

where $C_T$ is the total capacitance, $Q_T$ is the total electric charge, $R_{SC}$ is the SC internal resistance, $i_{SC}$ is the SC current, $N_s$ is the number in series, $N_p$ is the number in parallel, $C_H$ and $C_{GC}$ are the Helmholtz and Gouy–Chapman capacitance, $N_e$ is the number of electrode layers, $\varepsilon$ and $\varepsilon_0$ are the permittivity values of the electrolyte material and free space, $A_i$ is the interfacial area between electrodes and electrolyte, $d$ is the Helmholtz layer length, $Q_c$ is the cell electric charge, and $c$ is the molar concentration. In order to validate the SC model, a comparison test with commercial Maxwell BMOD SC, which is specifically designed for high-power transport

http://dx.doi.org/10.5772/64696

applications such as locomotive and the tramway, has been carried out in [20]. The validity of this model has been verified by experimental studies. The detailed description about the modeling of the SC model can be found in [6, 7, 20].

### 3.3. Modeling of DC/DC converters

A power electronic device is composed of a PWM-based DC/DC converter for each power source, which connects the sources with the DC bus. The PEMFC, battery, and SC present a lower terminal voltage than the DC voltage necessary to feed the traction inverter. Two unidirectional boost DC/DC converters have been developed by using the two-quadrant chopper models included in SimPowerSystems of Simulink [24, 25]. These converter connects two PEMFC systems with the 750VDC bus maintaining the PEMFC systems stable despite variations in load. Two bidirectional converters are, respectively, utilized to the batteries and the SCs with boost operation if discharging and buck operation if charging. These converter models also been developed by using the two-quadrant chopper models included in SimPowerSystems [24, 25]. The batteries and the SCs are located on the low-voltage side, and the high-voltage side is connected to the 750VDC bus. Therefore, the effective control of the duty cycle of the bidirectional converters assure the rated voltage of the DC bus and the charge and discharge safety of the batteries and the SCs.

## 4. Energy management strategies for hybrid tramway

### 4.1. A state machine strategy based on droop control

A droop control approach is presented to coordinate multiple motor and trailer units (multiple power sources), which is responsible for determining the reference power command to match the load requests from a driving cycle of tramway [7]. A reference power $P_{\text{ref}}$ versus bus voltage $U_{\text{bus}}$ droop is adopted. This characteristic is designed to convert the external command voltage $U_{\text{dcref}}$ = 750 V into the reference power $P_{\text{ref}}$. The larger is the amount of reference power that is injected or absorbed, the lower of the bus voltage is allowed to sag compared to the external request. Conversely, $P_{\text{ref}}$ is allowed to swell as the power is injected or absorbed. This correction successfully limits the circulating currents because it limits the power injections or absorptions to achieve the adjusted voltages. It is responsible for modifying the value of the bus voltage. The droop characteristic is realized by multiplying the droop coefficient m with the voltage error for the reference power, which is expressed as follows:

$$P_{\text{ref}} = \begin{cases} P_{\text{reflimt1}} & U_{\text{bus}} > U_{\text{H2}} \\ m(U_{\text{bus}} - U_{\text{dcref}} - \Delta U) & U_{\text{H1}} < U_{\text{bus}} < U_{\text{H2}} \\ 0 & U_{\text{L1}} < U_{\text{bus}} < U_{\text{H1}} \\ m(U_{\text{dcref}} - \Delta U - U_{\text{bus}}) & U_{\text{L2}} < U_{\text{bus}} < U_{\text{L1}} \\ P_{\text{reflimt2}} & U_{\text{bus}} < U_{\text{L2}} \end{cases} \tag{8}$$

where $U_{L2}$ and $U_{H2}$ are upper and lower voltage threshold based on $P_{reflimit1}$ and $P_{reflimit2}$, and $U_{L1}$ and $U_{H1}$ are upper and lower voltage threshold of active power sources. The droop coefficient $m$ determines the slopes of the droop characteristics, and it depends on the values of $m_a$, $m_b$, $k_1$, $k_2$, $SOC_{bat\_i}$, and $SOC_{sc\_i}$ ($i = 1 \ldots n$, $n$ is the numbers of batteries or SC), which is defined as follows:

$$m = \begin{cases} \dfrac{m_a}{k_1 \dfrac{\sum_{i=1}^{n} SOC_{bat\_i}}{n} + k_2 \dfrac{\sum_{i=1}^{n} SOC_{sc\_i}}{n}} & U_{H1} < U_{bus} < U_{H2} \\ m_b \left( k_1 \dfrac{\sum_{i=1}^{n} SOC_{bat\_i}}{n} + k_2 \dfrac{\sum_{i=1}^{n} SOC_{sc\_i}}{n} \right) & U_{L1} < U_{bus} < U_{L2} \end{cases} \tag{9}$$

Furthermore, the state machine strategy based on droop control (SMS-DC) is developed for the hybrid tramway. The aim of the SMS-DC is to decide the PEMFC reference power with the state change. Five states designed by the SMS are defined to distribute the reference power signals $P_{fcref}$, $P_{batref}$, and $P_{scref}$ for the PEMFC, the battery and the SC through regulating two unidirectional DC/DC converters, and four bidirectional DC/DC converters. $SOC_{batmin}$ and $SOC_{batmax}$ are the lower and the upper limits of battery SOC; $SOC_{scmin}$ and $SOC_{scmax}$ are the lower and the upper limits of SC SOC; $SOC_{batnom1}$ and $SOC_{batnom2}$ are the upper and lower bounds of the preferred zone of battery SOC; and $SOC_{scnom1}$ and $SOC_{scnom2}$ are the upper and lower bounds of the preferred zone of SC SOC. And also, the SOC levels of batteries and SCs are divided into the high SOC, normal SOC and low SOC, and the changes between these levels are performed by means of two hysteresis cycles. The state chart diagram of the SMS is described as **Figure 3** shown. The PEMFC reference power $P_{fcref}$ is determined based on the batteries and SCs SOC range and the reference power derived from droop control. In addition, the reference signal is decided for energy dissipation via the braking resistor if required during regenerative braking. These states are defined as follows:

State 1:

$$P_{fcref\_i} = \begin{cases} P_{fcmax} & if\ P_{ref} \geq nP_{fcmax} + P_{aux} \\ P_{ref}/n & if\ nP_{fcmax} + P_{aux} > P_{ref} \geq nP_{fcmin} + P_{aux} \\ P_{fcmin} & if\ nP_{fcmin} + P_{aux} > P_{ref} \end{cases} \tag{10}$$

State 2:

$$P_{fcref\_i} = P_{fcpre\_i} \tag{11}$$

State 3:

http://dx.doi.org/10.5772/64696

$$P_{\text{fcref\_i}} = \begin{cases} P_{\text{fcmax}} & if\ P_{\text{ref}} \geq nP_{\text{fcmax}} + P_{\text{aux}} \\ P_{\text{ref}}/n & if\ nP_{\text{fcmax}} + P_{\text{aux}} > P_{\text{ref}} \geq nP_{\text{fcopt}} + P_{\text{aux}} \\ P_{\text{fcopt}} & if\ nP_{\text{fcopt}} + P_{\text{aux}} > P_{\text{ref}} \end{cases} \tag{12}$$

State 4:

$$P_{\text{fcref\_i}} = P_{\text{fcpre\_i}} \tag{13}$$

State 5:

$$P_{\text{fcref\_i}} = \begin{cases} P_{\text{fcmax}} & if\ P_{\text{ref}} \geq nP_{\text{fcmax}} + P_{\text{aux}} \\ P_{\text{ref}}/n + P_{\text{char}} & if\ nP_{\text{fcmax}} + P_{\text{aux}} \geq P_{\text{ref}} \end{cases} \tag{14}$$

where $P_{\text{fcref\_i}}$ denotes the reference power of $i$-th PEMFC system, $P_{\text{fcmin}}$ and $P_{\text{fcmax}}$ are the lower and upper limits of PEMFC system, $P_{\text{aux}}$ is the auxiliary services power of tramway, $P_{\text{char}}$ is the minimum charging power of battery and SC, *and* $P_{\text{fcopt}}$ is the optimal power of PEMFC system.

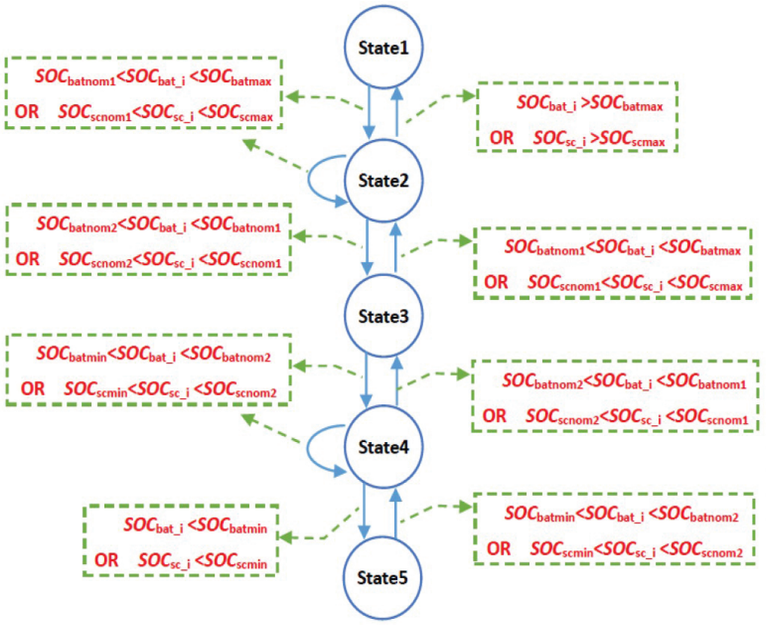


**Figure 3.** State chart diagram of the SMC-DC.

### 4.2. Energy management strategy based on fuzzy logic control

The fuzzy logic controller (FLC) is more appropriate for the energy management system of hybrid tramway. A list of IF-THEN rules is adopted to describe input and output relationship

of the controller [6]. In the fuzzy inference system, two decentralized FLC are designed improve the efficiencies of tramway and PEMFC systems on condition that dynamic property of tramway is satisfied.

The No. 1 FLC (FLC1) has three input variables and one output variable. The input variables include the demand power of electrical motor $P_{m1}$, the battery SOC, and the SC bank SOC (CSOC). The PEMFC reference power $P_{ref1}$ is defined as the output variable. The No. 2 FLC (FLC2) has three input variables and one output variable. The surplus demand power of motor $P_{m2}$, and the battery SOC and the SC CSOC are defined as the input variables. The SC reference power $P_{ref3}$ is defined as the output variable. The form of fuzzy reasoning is "IF $P_{m1}$ is $A_i$ AND SOC is $B_i$ AND CSOC is $C_i$, Then $P_{ref1}$ is $D_i$". Mamdani inference method is adopted to implement the fuzzy reasoning. More detailed description about the energy management strategy based on fuzzy logic control can be found in [6].

### 4.3. Equivalent consumption minimization strategy

In the present hybrid tramway, if the batteries or the SCs supply electrical energy, their SOC decreases, so that the batteries or the SCs will need to be recharged by the energy proceeded from two PEMFC systems or the tramway braking in order to maintain a desired SOC. Hence, extra hydrogen consumption could be needed due to the energy obtained from the tramway braking is generally insufficient. If the batteries or the SCs is recharged their SOC increases and the energy will supply to the tramway in future accelerations or start-ups resulting in a reduction of the hydrogen consumption. The electrical energy consumption of the batteries and the SCs are transformed into an equivalent hydrogen consumption to make the two comparable [10].

The equivalent consumption minimization strategy (ECMS) focuses on minimizing the equivalent hydrogen consumption of the hybrid powertrain $C$ (g), which is calculated as sum of two PEMFC systems hydrogen consumption $C_{fc}$, and two batteries and two SCs-equivalent hydrogen consumptions, $C_{bat}$ and $C_{sc}$. In this work, the mathematical problem used to optimize the equivalent hydrogen consumption is formulated as follows:

$$\begin{aligned} &min\ C = min\ \left(C_{fc} + \omega_1 C_{bat} + \omega_2 C_{sc}\right) \\ &subject\ to \begin{cases} SOC_{batmin} \le SOC_{bat\_i} \le SOC_{bat\,max} \\ SOC_{sc\,min} \le SOC_{sc\_i} \le SOC_{sc\,max} \\ P_{reflimt\,1} \le P_{ref} \le P_{reflmit\,2} \end{cases} \end{aligned} \tag{15}$$

where $\omega_1$ and $\omega_2$ is the penalty coefficients, which modifies the batteries and the SCs-equivalent hydrogen consumption up or down depending on their SOC deviation from the target. This optimization problem is subject to the constrains of the batteries and the SCs charging-sustaining and the power level. In addition, since the aim of two SCs is to provide the power peaks demanded by the hybrid tramway during the acceleration or braking that two PEMFC

http://dx.doi.org/10.5772/64696

systems and two batteries cannot generate or absorb, their average value will be minimum and $C_{sc}$ can be neglected compared with $C_{fc}$ and $C_{bat}$. Hence, $\omega_2$ is set to zero here, and $\omega_1$ limited by $\mu$ and the boundary of SOC is expressed as follows:

$$\omega_1 = 1 - 2\mu \frac{\left[SOC_{\text{bat\_i}} - 0.5\left(SOC_{\text{batmax}} + SOC_{\text{batmin}}\right)\right]}{SOC_{\text{batmax}} - SOC_{\text{batmin}}} \tag{16}$$

The battery-equivalent hydrogen consumption $C_{bat}$ can be calculated from the battery power $P_{bat}$. This concept is developed in [10, 11], where the battery charging and discharging efficiencies are calculated based on the equivalent internal resistance model. The battery-equivalent hydrogen consumption $C_{bat}$ can be expressed as follows:

$$C_{\text{bat}} = \begin{cases} \dfrac{P_{\text{bat}}}{\eta_{\text{chavg}}} \dfrac{C_{\text{fcavg}}}{P_{\text{fcavg}}} \left( \dfrac{1}{2} + \dfrac{1}{2} \sqrt{1 - \dfrac{4R_{\text{dis}} P_{\text{bat}}}{E^2}} \right)^{-1} & P_{\text{bat}} \geq 0 \\ P_{\text{bat}} \eta_{\text{disavg}} \dfrac{C_{\text{fcavg}}}{P_{\text{fcavg}}} \left( \dfrac{1}{2} + \dfrac{1}{2} \sqrt{1 - \dfrac{4R_{\text{ch}} P_{\text{bat}}}{E^2}} \right)^{-1} & P_{\text{bat}} < 0 \end{cases} \tag{17}$$

where $\eta_{chavg}$ and $\eta_{disavg}$ are the mean efficiencies of the battery charging and discharging, respectively, $C_{fcavg}$ is the average hydrogen consumption of the PEMFC systems, $P_{fcavg}$ is the average power of the PEMFC systems, *and* $R_{ch}$ and $R_{dis}$ are the resistances of the battery charging and discharging, respectively. The analytic solution to the optimized problem defined in Eq. (16) can be expressed as follows:

$$P_{\text{batop}} = \begin{cases} U_{\text{batmin}} \left(E - U_{\text{batmin}}\right) / R_{\text{dis}} & K_3 \leq x_{\min} \\ E^2 \left(1 - K_3^2\right) / 4R_{\text{dis}} & x_{\min} < K_3 \leq 1 \\ 0 & 1 < K_3 \leq 1 / \left(\eta_{\text{chavg}} \eta_{\text{disavg}}\right) \\ E^2 \left[1 - \left(K_3 \eta_{\text{chavg}} \eta_{\text{disavg}}\right)^2\right] / 4R_{\text{dis}} & 1 / \left(\eta_{\text{chavg}} \eta_{\text{disavg}}\right) < K_3 \leq x_{\max} / \left(\eta_{\text{chavg}} \eta_{\text{disavg}}\right) \\ -U_{\text{batmax}} \left(U_{\text{batmax}} - E\right) / R_{\text{ch}} & K_3 \geq x_{\max} / \left(\eta_{\text{chavg}} \eta_{\text{disavg}}\right) \end{cases} \tag{18}$$

where $P_{batopt}$ is the optimized power of the battery, *and* $U_{batmin}$ and $U_{batmax}$ are the minimal and the maximal allowed battery voltages, respectively. $K_1$, $x_{min}$, *and* $x_{max}$ are defined variables. In addition, since the aim of two SCs is to provide the power peaks demanded by the hybrid tramway during the acceleration or braking that two PEMFC systems and two batteries cannot generate or absorb, their average value will be minimum and $C_{sc}$ can be neglected compared with $C_{fc}$ and $C_{bat}$.

## 5. Results and discussions

A real driving cycle of the tramway from Samsun in Turkey is adopted to evaluate the performance of these energy management strategies for the hybrid system. A round-trip route, which consists of a symmetrical route of going and return, has been adopted as shown in **Figure 4**. The hybrid propulsion system of tramway is composed of commercial devices, such as Ballard FCvelocity™ HD6, Microvast Battery MV06203127NTPCA, and Maxwell BMOD0615. The premises are considered carefully for the hybrid system sizing. The maximum power of two PEMFC systems should be higher than the average power demanded by the tramway during the driving cycle in order to avoid excessive SOC drop of the batteries and the SCs. A hybrid propulsion system considered for the tramway presents two PEMFC systems (300 kW), two Li-ion batteries (40 Ah), and two SC banks (45 F). These devices have been selected from commercially available components as **Table 1** shown.

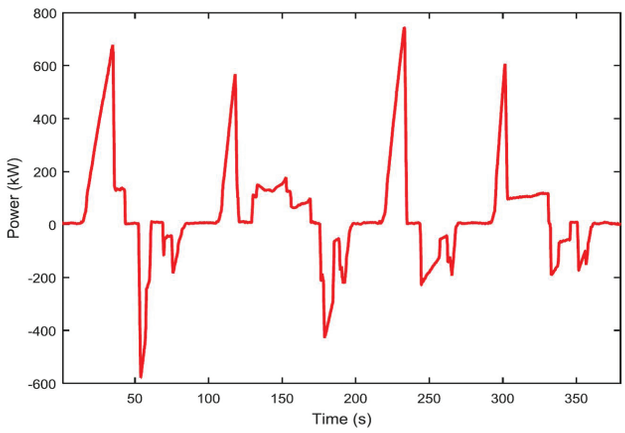


**Figure 4.** Driving cycle of hybrid tramway.

| | | | |
|---|---|---|---|
| *PEMFC* | | | |
| Manufacturer | Ballard stack modules-FCvelocity™ HD6 | | |
| Rated power (kW) | 260 | Rated voltage range (V) | 570–650 |
| Nominal coolant temperature (°C) | 50-63 | Mass (kg) | 710 |
| Maximum coolant temperature (°C) | 66 | Set numbers | 2 parallel |
| *Li-ion Battery* | | | |
| Manufacturer | Microvast battery MV06203127NTPCA | | |
| Capacity (Ah) | 40 | Rated voltage (V) | 331 |
| Maximum discharging rate (C) | 5 | Set numbers | 2 parallel |
| Maximum discharging current (a) | 240 | Mass (kg) | 280 |
| *Supercapacitor (SC)* | | | |
| Manufacturer | Maxwell BMOD0615 | | |
| Capacity (F) | 45 | Rated voltage (V) | 528 |
| Absolute maximum current (A) | 1400 | Specific power (W/kg) | 3300 |
| Set numbers | (11 series * 3 parallel) * 2 parallel | Mass (kg) | 670 |

**Table 1.** Parameters of commercial devices.

http://dx.doi.org/10.5772/64696

The performance comparison of these energy management strategies are carried out under the same the driving cycle and hybrid topology. In **Table 2**, the criteria for performance comparison are the average efficiency and equivalent hydrogen consumptions of tramway, the average value of $SOC_{bat}$ and $SOC_{sc}$, and the variation range of $SOC_{bat}$ and $SOC_{sc}$. Compared with the other strategies, the SMS-DC provides better tramway average efficiency (56.78%) and the tramway-equivalent hydrogen consumptions (301.22 g). The maximum difference obtained between the best and the worst tramway average efficiency is 7.7%. The efficient use of the batteries and SCs energy (average SOC of 75.12 and 78.02%) are also achieved by the SMS-DC because the final average SOC value of batteries and SCs are closer to the initial value. The best results related to the variation ranges of $SOC_{bat}$ and $SOC_{sc}$ are obtained by the ECMS, but at the expense of lower overall efficiency (49.72%).

| **EMS** | | | |
|---|---|---|---|
| **Criteria** | **FLC** | **ECMS** | **SMS-DC** |
| Tramway average efficiency (%) | 49.08 | 49.72 | 56.78 |
| Tramway-equivalent hydrogen consumptions (g) | 413.69 | 325.71 | 301.22 |
| Average $SOC_{bat}$ (%) | 73.37 | 73.56 | 75.12 |
| Average $SOC_{sc}$ (%) | 79.08 | 77.92 | 78.02 |
| $SOC_{bat}$ range | [70, 77] | [73, 76] | [72, 76] |
| $SOC_{sc}$ range | [55, 92] | [63, 80] | [57, 82] |

**Table 2.** Results of different strategies.

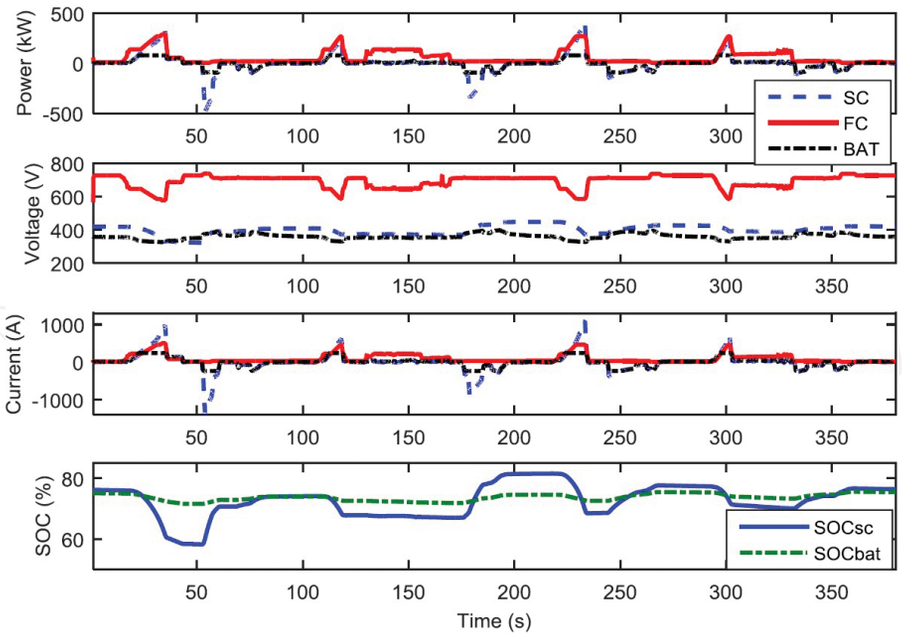


**Figure 5.** Output power, voltage, current, and SOC of different power sources.

As the results of the energy management system based on the SMS-DC, the output power, voltage, current, and SOC of different power sources are given in **Figure 5**, respectively. With

regard to the output power, the PEMFC systems only increase or decrease the power during high accelerations or brakings. It can be observed that the proposed SMS based on droop control is able to guarantee the stable operation of the PEMFC systems during the most of the drive cycle. The output power of the batteries alternates between negative and positive according to charging or discharging. It helps provide a portion of the positive low-frequency components of power demand to reduce the burden of the PEMFC and absorb the slow-variation negative portion. Additionally, due to the PEMFC dynamic limitation, the SCs provide the transient power demand successfully during sudden acceleration or braking. Their fast response fulfill the power demand, increase the hybrid system power density, and have to generate or absorb the power, which, either the PEMFC or the battery, are not able to generate or absorb.

## 6. Conclusions

In this chapter, the energy management system for the hybrid tramway based on multiple PEMFC systems, batteries, and SCs is designed without grid connection. The hybrid propulsion system model is developed with commercially available devices. The FLC, the ECMS, and the SMS-DC are utilized to coordinate and distribute the power demand to each power source appropriately, avoid the transients and rapid changes of power demand, and achieve high efficiency. According to the driving cycle of the tramway, the testing of the energy management systems is carried out. The comparisons with the FLC, the ECMS, and the SMS-DC verify that the higher average efficiencies of the tramway, the lower tramway-equivalent hydrogen consumptions, and more efficient use of the batteries and SCs energy are achieved by the SMS-DC. Hence, the suitable designed energy management system for the hybrid tramway will enhance the hydrogen consumptions of overall hybrid system and the efficiencies of each power source.

## Acknowledgements

This work was supported by National Natural Science Foundation of China (51177138, 61473238, 51407146), National Key Technology R&D Program (2014BAG08B01), and Sichuan Provincial Youth Science and Technology Fund (2015JQ0016).

## Author details

Qi Li* and Weirong Chen

*Address all correspondence to: liqi0800@163.com

School of Electrical Engineering, Southwest Jiaotong University, Chengdu, China

## References

[1] O. Erdinc, M. Uzunoglu. Recent trends in PEM fuel cell-powered hybrid systems: investigation of application areas, design architectures and energy management approaches. Renew. Sustain. Energy Rev. 2010;14:2874–2884. doi:10.1016/j.rser.2010.07.060.

[2] C. Bao, M. Ouyang, B. Yi. Modeling and control of air stream and hydrogen flow with recirculation in a PEM fuel cell system-II. Linear and adaptive nonlinear control. Int. J. Hydrogen Energy. 2006;31:1897–1913. doi:10.1016/j.ijhydene.2006.02.030.

[3] Q. Li, W. Chen, Y. Li, S. Liu, J. Huang. Energy management strategy for fuel cell/battery/ultracapacitor hybrid vehicle based on fuzzy logic. J. Electrical Power Energy Syst. 2012;43:514–525. doi:10.1016/j.ijepes.2012.06.026.

[4] J. Jia, G. Wang, Y.T. Cham, Y. Wang, M. Han. Electrical characteristic study of a hybrid PEMFC and ultracapacitor system. IEEE Trans. Ind. Electron. 2010;57:1945–1953. doi:10.1109/TIE.2009.2022066.

[5] L. Xu, J. Li, M. Ouyang, J. Hua, G. Yang. Multi-mode control strategy for fuel cell electric vehicles regarding fuel economy and durability. Int. J. Hydrogen Energy. 2014;39:2374–2389. doi:10.1016/j.ijhydene.2013.11.133.

[6] Q. Li, W. Chen, Z. Liu, M. Li, L. Ma. Development of energy management system based on a power sharing strategy for a fuel cell–battery–supercapacitor hybrid tramway. J. Power Sources. 2015;279:267–280. doi:10.1016/j.jpowsour.2014.12.042.

[7] Qi Li, Hanqing Yang, Ying Han, Ming Li, Weirong Chen. A State Machine Strategy based on Droop Control for an Energy Management System of PEMFC-Battery-Supercapacitor Hybrid Tramway. Int. J. Hydrogen Energy. 2016;41: 12705–12713. DOI: 10.1016/j.ijhydene.2016.04.254.

[8] F. Peng, W. Chen, Z. Liu, Q. Li, C. Dai. System integration of China's first proton exchange membrane fuel cell locomotive. Int. J. Hydrogen Energy. 2014;39:13886–13893. doi:10.1016/j.ijhydene.2014.01.166.

[9] A.R. Miller, K.S. Hess, D.L. Barnes, T.L. Erickson. System design of a large fuel cell hybrid locomotive. J. Power Sources. 2007;173:935–942. doi:10.1016/j.jpowsour.2007.08.045.

[10] P. García, J.P. Torreglosa, L.M. Fernández, F. Jurado. Viability study of a FC–battery–SC tramway controlled by equivalent consumption minimization strategy. Int. J. Hydrogen Energy. 2012;37:9368–9382. doi:10.1016/j.ijhydene.2012.02.184.

[11] J.P. Torreglosa, F. Jurado, P. Garcı´a, L.M. Ferna´ndez. Hybrid fuel cell and battery tramway control based on an equivalent consumption minimization strategy. Control Eng. Pract. 2011;19:1182–1194. doi:10.1016/j.conengprac.2011.06.008.

[12] L.M. Fernandez, P. Garcia, C.A. Garcia, F. Jurado. Hybrid electric system based on fuel cell and battery and integrating a single dc/dc converter for a tramway. Energy Convers. Manag. 2011;52:2183–2192. doi:10.1016/j.enconman.2010.12.028.

[13] P. Thounthong, P. Tricoli, B. Davat. Performance investigation of linear and nonlinear controls for a fuel cell/supercapacitor hybrid power plant. J. Electrical Power Energy Systems. 2014;54:454–464. doi:10.1016/j.ijepes.2013.07.033.

[14] Y. Eren, O. Erdinc, H. Gorgun, M. Uzunoglu, B. Vural. A fuzzy logic based supervisory controller for an FC/UC hybrid vehicular power system. Int. J. Hydrogen Energy. 2009;34:8681–8694. doi:10.1016/j.ijhydene.2009.08.033.

[15] Q. Li, W. Chen, Z. Liu, A. Guo, J. Huang. Nonlinear multivariable modeling of locomotive proton exchange membrane fuel cell system. Int. J. Hydrogen Energy. 2014;39:13777–13786. doi:10.1016/j.ijhydene.2013.12.211.

[16] Q. Li, W. Chen, Z. Liu, A. Guo, S. Liu. Control of proton exchange membrane fuel cell system breathing based on maximum net power control strategy. J. Power Sources. 2013;214:212–218. doi:10.1016/j.jpowsour.2013.04.067.

[17] J.T. Pukrushpan, A.G. Stefanopoulou, H. Peng. Control of fuel cell breathing. IEEE Control Syst. Mag. 2004;24:30–46. doi:10.1109/MCS.2004.1275430.

[18] A. Arce, A.J. del Real, C. Bordons, D.R. Ramirez. Real-time implementation of a constrained MPC for efficient airflow control in a PEM fuel cell. IEEE Trans. Ind. Electron. 2010;57:1892–1905. doi:10.1109/TIE.2009.2029524.

[19] Q. Li, W. Chen, Y. Wang, J. Jia, M. Han. Nonlinear robust control of proton exchange membrane fuel cell by state feedback exact linearization. J. Power Sources. 2009;194:338–348. doi:10.1016/j.jpowsour.2009.04.077.

[20] S.N. Motapon, L.A. Dessaint, K. Al-Haddad. A comparative study of energy management schemes for a fuel-cell hybrid emergency power system of more-electric aircraft. IEEE Trans. Ind. Electron. 2014;61:1320–1334. doi:10.1109/TIE.2013.2257152.

[21] T.C. Yang. Initial study of using rechargeable batteries in wind power generation with variable speed induction generators. IET Renew. Power Gener. 2008;2:89–101. doi:10.1049/iet-rpg:20070008.

[22] G. Sikha, R.E. White, B.N. Popov. A mathematical model for a lithium-ion battery/electrochemical capacitor hybrid system. J. Electrochem. Soc. 2005;152:1682–1693. doi:10.1149/1.1940749.

[23] K.B. Oldham. A Gouy-Chapman-Stern model of the double layer at a (metal)/(ionic liquid) interface. J. Electroanal. Chem. 2008;613:131–138. doi:10.1016/j.jelechem.2007.10.017.

[24] M. Delshad, H. Farzanehfard. A new soft switched push pull current fed converter for fuel cell applications. Energy Convers. Manag. 2011;52:232–243. doi:10.1016/j.enconman.2010.08.019.

[25] D.D. Marquezini, D.B. Ramos, R.Q. Machado, F.A. Farret. Interaction between proton exchange membrane fuel cells and power converters for AC integration. IET Renew. Power Gener. 2008;2:151–161. doi:10.1049/iet-rpg:20070057.



IntechOpen

IntechOpen